Laser Photonics Rev. **7,** No. 6, L77–L83 (2013) / **DOI** 10.1002/lpor.201300084

LASER & PHOTONICS REVIEWS

Abstract Topological insulators are states of quantum matter that have narrow topological nontrivial energy gaps and a large third-order nonlinear optical response. The optical absorption of topological insulators can become saturated under strong excitation. In this work, with Bi_2Se_3 as an example, it was demonstrated that a topological insulator can modulate the operation of a bulk solid-state laser by taking advantage of its saturable absorption. The result suggests that topological insulators are potentially attractive as broadband pulsed modulators for the generation of short and ultrashort pulses in bulk solid-state lasers, in addition to other promising applications in physics and computing.

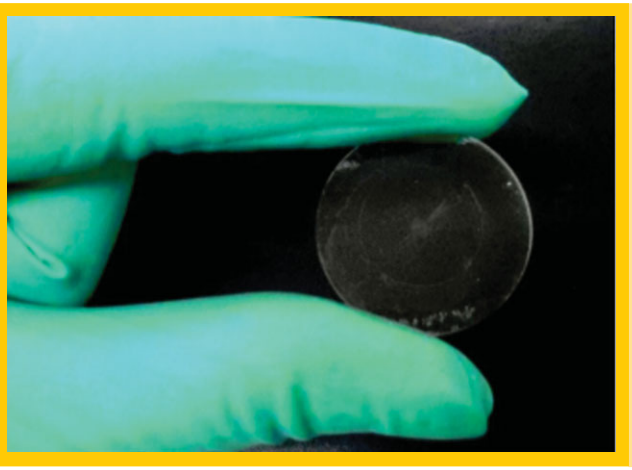

LETTER ARTICLE

Topological insulator as an optical modulator for pulsed solid-state lasers

Haohai Yu[1,], Han Zhang[2,**], Yicheng Wang[1], Chujun Zhao[2], Baolin Wang[1], Shuangchun Wen[2], Huaijin Zhang[1,*], and Jiyang Wang[1]**

1. Introduction

Topological insulators are novel quantum electronic materials whose edge modes have exotic spin and charge properties [1–4]. At an edge or on a surface, the metallic state appears and is protected by the topological symmetry, such as time-reversal or crystalline symmetry [5, 6], which generates a bulk gap and an odd number of relativistic Dirac fermions on the surface [7]. Therefore, topological insulators behave as insulators in their interior but their surfaces contain metallic states [8]. These states allow electrons to travel on the surface of the material at room temperature, an effect that has promising applications in computing [9]. In recent years, exotic properties, including spin-orbit coupling, the quantum spin Hall effect, dissipationless spin current and the magnetoelectric effect have been investigated [4, 10–13]. A topological insulator has a single Dirac cone on the surface around the Γ point and a gap of 0.2–0.3 eV in the bulk [2, 14]. Thus, a topological insulator should also exhibit saturable absorption effect because of its narrow gap [15, 16], which means that, under weak excitation, the linear absorption of light dominate, while under strong excitation, the nonlinear absorption occurs. Based on the photoelectric effect, both the surface and bulk can absorb light and reach saturation under strong excitation when the wavelength of the incident light is shorter than 4.1 μm (0.3 eV).

The saturable absorption of many well-known saturable absorbers, including Cr:YAG, semiconductor saturable absorber mirrors (SESAM), and GaAs, are wavelength sensitive. Recently, single-walled carbon nanotubes have also been used as saturable absorbers depending on diameter selectivity and benefiting from the presence of small bundles. The diameter of a single-walled carbon nanotube controls its bandgap. Broadband absorption becomes possible by using carbon nanotubes with a broad diameter distribution [15, 17]. The performance of a mode-locked fiber laser with a topological insulator saturable absorber has been studied [17]. In contrast to fiber lasers, which have large gain, the diode-pumped solid-state bulk lasers (DPSSBLs), including crystalline, ceramic and glass lasers, have a relatively low gain and represent another research regime [18]. Up to now, the pulse DPSSBLs have been applied in many fields, such as industry, medicine, military applications, and basic scientific research, where compact, reliable, and cost-effective pulse lasers are required. Investigation on the possibility of using topological insulators as an optoelectronic device in DPSSBLs is attractive. In this paper, with Bi_2Se_3 as an example, we report on the investigation of a DPSSBL modulated by a topological insulator. The results

[1] State Key Laboratory of Crystal Materials and Institute of Crystal Materials, Shandong University, Jinan 250100, China
[2] Key Laboratory for Micro-/Nano-Optoelectronic Devices of Ministry of Education, College of Physics and Microelectronic Science, Hunan University, Changsha 410082, China
[**] These authors contributed equally to this work.
[*] Corresponding author: e-mail: huaijinzhang@sdu.edu.cn

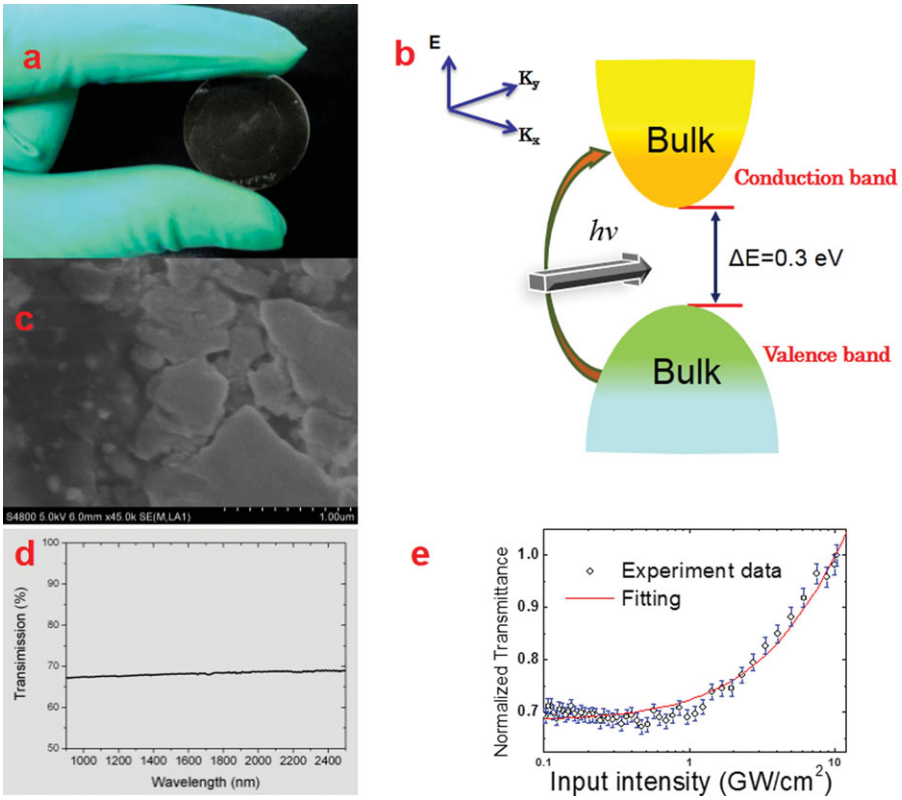

Figure 1 (a) Photograph of topological insulator Bi_2Se_3 sample on quartz substrate. (b) Simple schematic of excitation process responsible for light absorption in a topological insulator by considering the $\Delta E = 0.3$ eV gap in the bulk. The orange region indicates the bulk conduction band and the green region indicates the bulk valence band. (c) SEM image of Bi_2Se_3 on quartz substrate. (d) Absorbance of Bi_2Se_3 on quartz substrate. (e) Theoretical (red curve) and experimental (blue rings) power-dependent nonlinear transmittance of Bi_2Se_3 sample.

confirm the feasibility of using topological insulators as a saturable absorber for the generation of short and ultrashort pulses in DPSSBLs.

2. Results and discussion

2.1. Topological insulator modulator

The Bi_2Se_3 topological insulator plates used in the experiments were synthesized via a polyol method. A solution with dispersed Bi_2Se_3 was dropped onto a 1-mm thick quartz plate whose diameter was about 1 inch. The dried plate with the topological insulator on it is shown in Fig. 1a. Previous theoretical studies have shown that the Bi_2Se_3 electronic band structure possesses a one-valley conduction-band minimum and a one-valley valence-band maximum occurring at the center of the Brillouin zone, with a gap of 0.2–0.3 eV in the bulk and zero gap on the surface [19, 20]. When the wavelength of excitation light is shorter than 4.1 μm, corresponding to 0.3 eV per photon, both the surface and the bulk absorb light, and can be saturated under strong excitation. However, when the wavelength of excitation light is longer than 4.1 μm, the single Dirac cone on the surface responds with a nonlinear and saturable absorption. As shown by a previous theoretical calculation [2], the surface bandgap disperses in the bulk gap, and the gaps are almost uninfluenced by each other, in contrast to a traditional semiconductor whose bandgaps are influenced by the environment. An SEM image of a typical Bi_2Se_3 sample on a quartz substrate is presented in Fig. 1c. From this figure, it is seen that the Bi_2Se_3 plates are randomly distributed on the quartz on a micrometer scale, which indicates that most of the Bi_2Se_3 is in bulk form and the surface states generated on the edges or its surface [2] are relatively rare. Therefore, the linear and nonlinear optical absorption appears as the collective result of the bulk and surface states, and absorption by the Bi_2Se_3 sample can mainly be attributed to the narrow gap in the bulk. Figure 1b shows the excitation process responsible for light absorption in the topological insulator Bi_2Se_3 with a 0.3 eV bulk gap corresponding to a light wavelength of 4.1 μm. A photon can excite an electron from the valence band to the conduction band when the light wavelength is shorter than 4.1 μm. Using the semiconductor two-level model [21], under strong light excitation, electrons from the valence band (green) are excited into the conduction band (orange) and the states in the valence band become depleted, while the finial states in the conduction band are partially occupied. Further excitation from the valence band is blocked and no further absorption is induced, leading to a saturable absorption condition [15, 21]. Therefore, low (large) intensity light experiences large (low) loss, and the topological insulator can be used as a saturable absorber. For a short period of time after excitation, intraband phonon scattering and electron–hole recombination relax the photoexcited carriers as in graphene and semiconductor saturable absorbers [15, 21]. Shortly after that, however, the topological insulator absorbs light again. Due to the narrow gap in the bulk,

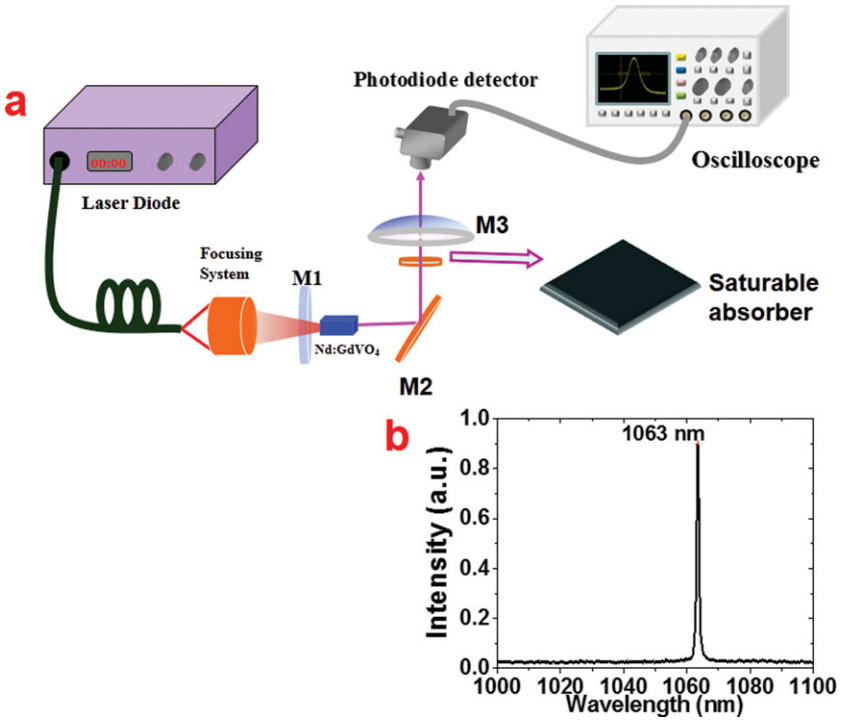

Figure 2 (a) Experimental setup of Nd:$GdVO_4$ pulsed laser. (b) Wavelength of the continuous-wave and pulsed lasers.

the topological insulator Bi_2Se_3 can be used as a broadband modulator in lasers with wavelengths shorter than 4.1 μm.

The X-ray diffraction (XRD) pattern is shown in Fig. 1b of Ref.17. This indicates that the Bi_2Se_3 sample used in the experiment has a rhombohedral structure (JCPDS card No.33-0214). The transmission spectrum of the sample is presented in Fig. 1d, which shows that the optical transmittance is about 68% over the wavelength range from 900 to 2500 nm. Considering the reflection of the quartz plate to be about 7%, the linear absorption of the sample is thus about 25%. The saturable absorption of Bi_2Se_3 induced by the imaginary part of the complex third-order susceptibility of the material is directly related to the photocarrier density. It can be described by the two-level saturable absorber model that is widely used for two-dimensional quantum wells and graphene:

$$\alpha^* = \frac{\alpha_s^*}{1 + \frac{N}{N_{sat}}} + \alpha_{NS}, \tag{1}$$

where α_s^* is the saturable and α_{NS} is the nonsaturable loss determined by the saturable and nonsaturable absorption coefficient, N is the photoinduced electron–hole density, and N_{sat} is the saturable density, which is the value of N where the absorption falls to one-half of its initial value. The photocarrier density can be simplified by introducing the incident light intensity (I) of a continuous-wave (cw) or long-pulse excitation as follows:

$$\begin{aligned} N &= \frac{\alpha^* I \tau}{\hbar\omega} \\ N_s &= \frac{\alpha^* I_s \tau}{\hbar\omega} \end{aligned}, \tag{2}$$

where τ is the carrier recombination time and ω is the light frequency. Under weak excitation, the absorption loss is $\alpha^* = \alpha_s^* + \alpha_{NS}^*$ and saturable absorption takes effect under strong excitation. Based on previous investigations [22,23], the carrier interband scattering time in the Bi_2Se_3 bulk conduction band is about 0.5 ps, while the relaxation time for the Dirac cone nonequilibrium electrons to recover a Fermi–Dirac distribution of the surface states is over 10 ps. However, the surface states disperse into bulk states and the relaxation time of the Bi_2Se_3 charge carriers is thus mainly determined by interband scattering from the bulk conduction band whose recombination time is more efficient [23]. The saturable absorption can therefore be expressed as:

$$\alpha^* = \frac{\alpha_s^*}{1 + \frac{I}{I_{sat}}} + \alpha_{NS} \tag{3}$$

and the saturation intensity I_{sat} describing the saturable photoinduced electron-hole density is the degree of difficulty of being fully saturated and the most important parameter to consider for saturable absorption. With the relationship between absorption and transmission, the power-dependent nonlinear transmittance of the Bi_2Se_3 sample can be fitted with the following formula [14, 17]:

$$T = A \exp\left(\frac{-\delta T}{1 + \frac{I}{I_{sat}}}\right), \tag{4}$$

where T is the transmission, A is a normalization constant and δT is the absolute modulation depth. The power-dependent nonlinear absorption of the Bi_2Se_3 sample was investigated using a mode-locked Ti-Sapphire laser. Based on Eq. (4), the relation between the normalized optical transmittance and incident optical power is presented in Fig. 1e. The normalized transmittance increases nonlinearly with incident pump power, and the normalized

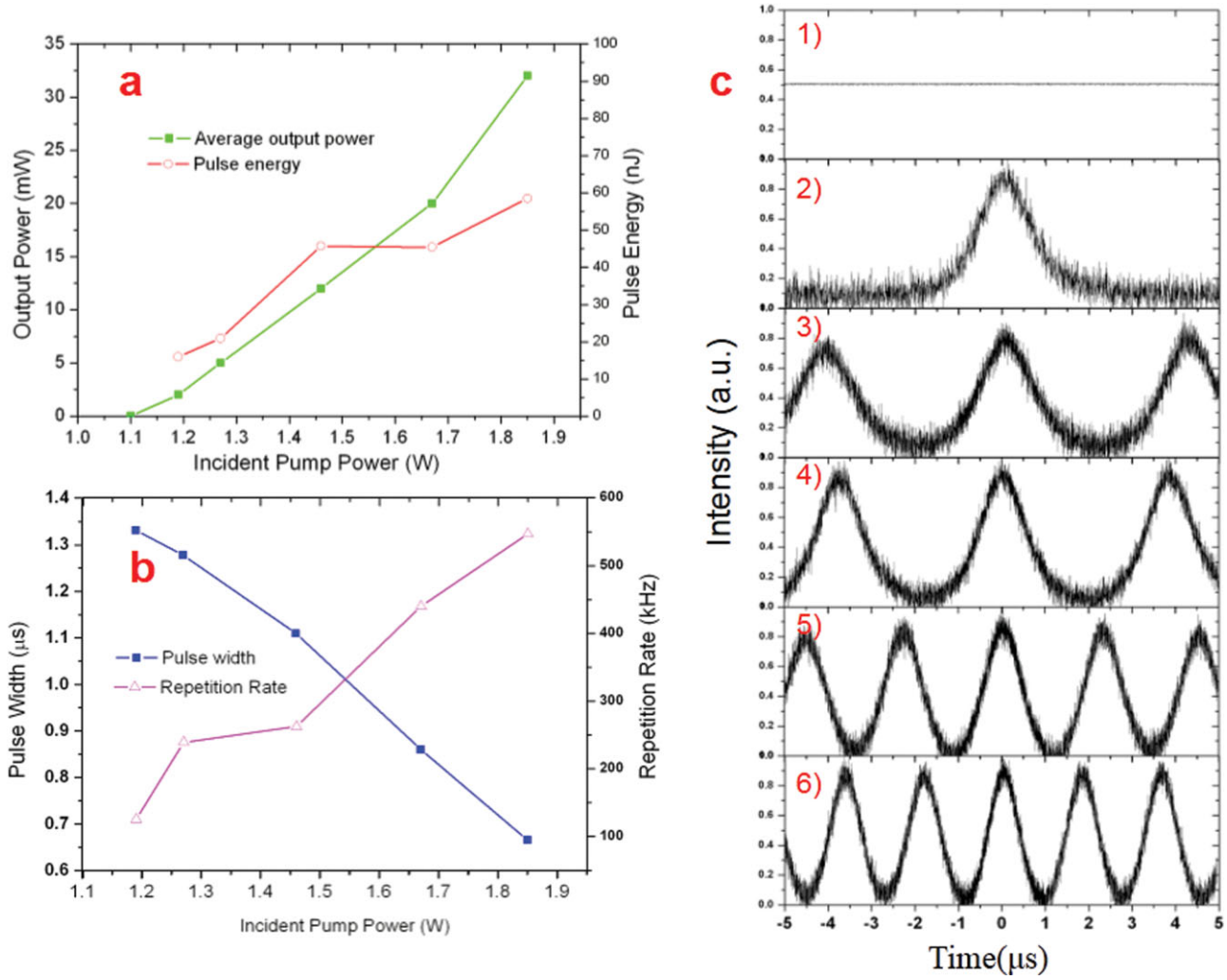

Figure 3 (a) Average output power and pulse energy vs. increasing incident pump power. (b) Pulse width and repetition rate vs. incident pump power. (c) Display recorded by digital oscilloscope for lasers. 1–6 Pulse profiles of continuous-wave Nd:$GdVO_4$ laser and pulsed lasers under pump power of 1.19 W, 1.27 W, 1.46 W, 1.67 W and 1.85 W, respectively.

modulation depth is 30%, which indicates that the Bi_2Se_3 sample exhibits saturable absorption. The saturation intensity was determined to be 4.3 GW/cm^2, a value that is much larger than that of graphene (0.71 to 0.61 MW/cm^2) [15], which indicates that the topological insulator Bi_2Se_3 is difficult to fully saturate and is more favorable to generating large-energy pulses as a Q-switcher based on the analysis of passively modulated pulsed lasers [21].

2.2. Passively modulated laser

To avoid damage and the effects caused by the unabsorbed pump power on the sample, an L-shaped cavity was used for constructing the pulse laser. The experimental laser setup is sketched in Fig. 2a, and its detailed description is given in the Section 4. By removing the saturable absorber from the cavity, a cw Nd:$GdVO_4$ laser was realized. The digital oscilloscope trace shown in Fig. 3c1) displays the cw laser emission. On inserting the saturable absorber into the laser cavity, passively Q-switched operation of the laser was obtained. The performance of the laser is shown in Fig. 3a. The Q-switching threshold was measured to be about 1.1 W and the output power increased quasilinearly with the pump power. The maximum output power reached 32 mW under an incident pump power of 1.85 W. The pulse width decreased, while the repetition rate increased with increase in the pump power, a result that is typical for a passively Q-switched laser [24]. The minimum pulse duration was 666 ns and the maximum repetition rate was 547 kHz. The variations of the pulse width and repetition rate with pump power are shown in Fig. 3b. Based on the measured average output power and repetition rate, the pulse energy was calculated, and shown in Fig. 3a. The maximum energy measured was 58.5 nJ.

Because the pulse energy increased with the incident pump power, we could conclude that the saturable absorber did not operate in the full-saturation regime, since the

oscillation intensity in the cavity remained low. Once the output power increased above 12 mW and the corresponding intracavity intensity reached a value higher than 60 mW, the pulse energy remained almost stable with respect to pump power, which suggests that the saturable absorber was almost totally saturated.

The digital oscilloscope trace of the laser output is displayed in Fig. 3c, and it can be seen that there were no pulse output by the cw laser. The pulse profile under a pump power of 1.19 W, 1.27 W, 1.46 W, 1.67 W and 1.85 W is shown in Figs. 3c 2–6, respectively. From this figure, it can be observed that the pulse trains were stable, the repetition rate increased with increasing pump power, and there was no mode locking. This result is different from what was observed in previous reports on fiber lasers [9]. It should also be noted that no thermal damage was observed on the surface of the topological insulator sample during the passively Q-switched laser operation, which indicates that a larger energy pulse can be modulated with Bi_2Se_3. From measurements with an optical spectrum analyser, the laser wavelength was found to be located at 1063 nm, as shown in Fig. 2b. Considering the previous results on fiber lasers at a wavelength of about 1.56 μm [17], the results presented here at a wavelength of 1.06 μm show that the topological insulator is also insensitive to excitation wavelength, as long as the wavelength is shorter than 4.1 μm. This result also demonstrates that the topological insulator can be used as a broadband optical material.

For passively Q-switched laser operation, the theoretical pulse width can be calculated using the following equation [25, 26]:

$$t = \frac{3.52T_{\mathrm{R}}}{\Delta T}, \tag{5}$$

where, T_{R} is the cavity round-trip time, and ΔT is the modulation depth. For our experimental conditions, $T_{\mathrm{R}} = 0.54$ ns, and therefore the maximum modulation depth ΔT is calculated to be less than 1%, which indicates that by increasing the modulation depth and improving the quality of the sample, the modulation properties of Bi_2Se_3 can be further improved.

3. Conclusions

A pulse bulk solid-state laser was constructed using a topological insulator, Bi_2Se_3 as the pulse modulator. These results demonstrate that the topological insulator is an effective broadband saturable absorber for pulse DPSSBLs with potential applications as broadband laser photonics. Comparative results on graphene, carbon nanotubes, and topological insulators for use as optical modulators in bulk lasers are shown in Table 1. By further optimizing the quality and modulation depth of the topological insulator, pulsed laser performance can be greatly improved. Besides promising applications in physics and computing, the easy fabrication and compactness in size, broadband modulation and the

Table 1 Comparative results on graphene, carbon nanotubes, and topological insulators as optical modulators in bulk lasers.

	Graphene					Carbon nanotube					Topological insulator				
	Wavelength					Wavelength					NA				
Mode-locking	0.8 μm	1 μm	1.5 μm	2 μm	2.5 μm	0.8 μm	1 μm	1.5 μm	2 μm	2.5 μm					
	63 fs (480 mW) [28]	160 fs (16 mW) [29]	91 fs (107 mW) [30]	410 fs (270 mW) [31]	226 fs (80 mW) [32]	62 fs (600 mW) [33]	100 fs (230 mW) [34]	92 fs [35]	175 fs (35 mW) [36]	NA					
	Wavelength					Wavelength									
Q-switching	0.8 μm	1 μm	1.5 μm	2μm	2.5 μm	NA					0.8 μm	1 μm	1.5 μm	2 μm	2.5 μm
	NA	56.2 ns (595.8 nJ) [37]	NA	1 μs, (1.74 μJ) [38]	NA						NA	666 ns (58.5 nJ) [This work]	NA	NA	NA

saturable absorption property augur a promising future in applications as an optoelectronic element.

4. Methods

4.1. Material preparation

The Bi_2Se_3 sample used in the experiments was synthesized via a polyol method [27]. The raw materials were $Bi(NO_3)_3{\cdot}5H_2O$, sodium selenite, polyvinyl pyrrolidone and ethylene glycol, all of which were added into a two-neck flask containing a Teflon-coated magnetic stirring bar. The solution was dropped onto a quartz plate, and the plate was then placed inside a drying oven for evaporation for 8 h. The product was washed with isopropyl alcohol several times.

4.2. Laser design

For the laser experiments, we used an L-shape resonator (see Fig. 2). The pump power was delivered through the plane mirror (M1), antireflection (AR) coated for the pump wavelength of 808 nm, and highly reflective (HR) for the laser wavelength at about 1.06 μm. The 45° folding mirror (M2) was a plane mirror, HR for the laser wavelength, and AR-coated for the pump radiation wavelength. M3 was the output coupler with a transmission of about 20% for the laser wavelength and a 100 mm radius of curvature. The length between M1 and M2 was 3.5 cm and the length between M2 and M3 was 4.6 cm. The pump source, a fiber-coupled, NA = 0.22, 200 μm core diameter diode laser had an emission wavelength of 808 nm. The active element was a 8-mm thick, *a*-cut, 0.5 at.% Nd:$GdVO_4$ crystal with an aperture of 3 × 3 (along *c*) mm^2. The crystal surfaces were AR coated at 808 nm and 1.06 μm. The crystal was mounted in a Cu holder with circulating water at 15 °C. The incident pump beam was focused to a 200-μm spot diameter on the crystal with a focusing system.

The laser output power was measured by a power meter (EPM 2000. Molectron Inc.). The temporal behavior of the Q-switched laser was recorded by a TGS 3052 digital oscilloscope (500-MHz bandwidth and 2.5-Gs/s sampling rate, Tektronix Inc.). The laser spectrum was measured with an optical spectrum analyzer (HR4000CG-UV-NIR, Ocean Optics Inc.).

Acknowledgements. The authors wish to thank Professor R. I. Boughton, Department of Physics and Astronomy of Bowling Green State University, for discussions and linguistic advice. This work is supported by the National Natural Science Foundation of China (No. 51025210, 91022034, 51272131 and 51102156) and the Program of Introducing Talents of Discipline to Universities in China (111 program).

Received: 18 June 2013, **Revised:** 11 September 2013, **Accepted:** 13 September 2013

Published online: 11 October 2013

Key words: Topological insulator, saturable absorption, pulsed solid-state bulk laser, passively Q-switching.

References

[1] J. E. Moore, Nature **464**, 194–198 (2010).
[2] H. J. Zhang, C. X. Liu, X. L. Qi, X. Dai, Z. Fang, and S. C. Zhang, Nature Phys. **5**, 438–442 (2009).
[3] B. A. Bernevig, T. L. Hughes, and S. C. Zhang, Science **314**, 1747–1761 (2006).
[4] C. L. Kane and E. J. Mele, Phys. Rev. Lett. **95**, 146802 (2005).
[5] X.-L. Qi and S.-C. Zhang, Rev. Mod. Phys. **83**, 1057–1110 (2011).
[6] Y. Tanaka, Z. Ren, T. Sato, K. Nakayama, S. Souma, T. Takahashi, K. Segawa, and Y. Ando, Nature Phys. **8**, 800–803 (2012).
[7] L. Fu, C. L. Kane, and E. J. Mele, Phys. Rev. Lett. **98**, 106803 (2007).
[8] M. Z. Hasan and C. L. Kane, Rev. Mod. Phys. **82**, 3045–3067 (2010).
[9] Y. L. Chen, J. G. Analytis, J. H. Chu, Z. K. Liu, S. K. Mo, X. L. Qi, H. J. Zhang, D. H. Lu, X. Dai, Z. Fang, S. C. Zhang, I. R. Fisher, Z. Hussain, and Z. X. Shen, Science **325**, 178–181 (2009).
[10] B. A. Bernevig, T. L. Hughes, and S. C. Zhang, Science **314**, 1757–1761 (2006).
[11] C. Xu and J. E. Moore, Phys. Rev. B **73**, 045322 (2006).
[12] X. L. Qi, T. L. Hughes, and S. C. Zhang, Phys. Rev. B **78**, 195424 (2008).
[13] D. Hsieh, D. Qian, L. Wray, Y. Xia, Y. S. Hor, R. J. Cava, and M. Z. Hasan, Nature **452**, 970–975 (2008).
[14] F. Bernard, H. Zhang, S. P. Gorza, P. Emplit, In Nonlinear Photonics, OSA Digest, paper NTh1A. 5.
[15] Q. L. Bao, H. Zhang, Y. Wang, Z. H. Ni, Y. L. Yan, Z. X. Shen, K. P. Loh, and D. Y. Tang, Adv. Funct. Mater. **19**, 3077–3083 (2009).
[16] Z. Sun, T. Hasan, F. Torrisi, D. Popa, G. Privitera, F. Wang, F. Bonaccorso, D. M. Basko, and A. C. Ferrari, ACS Nano. **4**, 803–810 (2010).
[17] F. Bonaccorso, T. Hasan, P. H. Tan, C. Sciascia, G. Privitera, G. Di Marco, P. G. Gucciardi, and A. C. Ferrari, J. Phys. Chem. C **114**, 17267–17285 (2010).
[18] C. J. Zhao, Y. H. Zou, Y. Chen, Z. T. Wang, S. B. Lu, H. Zhang, S. C. Wen, and D. Y. Tang, Opt. Exp. **20**, 27888–27895 (2012).
[19] R. L. Byer, Science **239**, 742–747 (1988).
[20] S. K. Mishrayz, S. Satpathyyz, and O. Jepsen, J. Phys.: Condens. Matter **9**, 461–470 (1997).
[21] U. Keller, Nature **424**, 831–838 (2003).
[22] J. Qi, X. Chen, W. Yu, P. Cadden-Zimansky, D. Smirnov, N. H. Tolk, I. Miotkowski, H. Cao, Y. P. Chen, Y. Wu, S. Qiao, and Z. Jiang, Appl. Phys. Lett. **97**, 182102 (2010).
[23] M. Hajlaoui, E. Papalazarou, J. Mauchain, G. Lantz, N. Moisan, D. Boschetto, Z. Jiang, I. Miotkowski, Y. P. Chen, A. Taleb-Ibrahimi, L. Perfetti, and M. Marsi, Nano Lett. **12**, 3532–3536 (2012).
[24] X. Zhang, S. Zhao, Q. Wang, Q. Zhang, L. Sun, and S. Zhang, IEEE J. Quantum. Electron. **33**, 2286–2294 (1997).

[25] G. J. Spühler, R. Paschotta, R. Fluck, B. Braun, M. Moser, G. Zhang, E. Gini, and U. J. Keller, Opt. Soc. Am. B **16**, 376–388 (1999).
[26] J. J. Zayhowski and P. L. Kelley, IEEE J. Quantum Electron. **27**, 2220–2225 (1991).
[27] J. Zhang, Z. P. Peng, A. Soni, Y. Y. Zhao, Y. Xiong, B. Peng, J. B. Wang, M. S. Dresselhaus, and Q. H. Xiong, Nano Lett. **11**, 2407–2414 (2011).
[28] I. H. Baek, H. W. Lee, S. Bae, B. H. Hong, Y. H. Ahn, D.-Il. Yeom, and F. Rotermund, Appl. Phys. Exp. **5**, 032701 (2012).
[29] E. Ugolotti, A. Schmidt, V. Petrov, J. W. Kim, D. Yeom, F. Rotermund, S. Bae, B. H. Hong, A. Agnesi, C. Fiebig, G. Erbert, X. Mateos, M. Aguil, F. Diaz, and U. Griebner, Appl. Phys. Lett. **101**, 161112 (2012).
[30] S. D. D. D. Cafiso, E. Ugolotti, A. Schmidt, V. Petrov, U. Griebner, A. Agnesi, W. B. Cho, B. H. Jung, F. Rotermund, S. Bae, B. H. Hong, G. Reali, and F. Pirzio, Opt. Lett. **38**, 1745–1747 (2013).
[31] A. A. Lagatsky, Z. Sun, T. S. Kulmala, R. S. Sundaram, S. Milana, F. Torrisi, O. L. Antipov, Y. Lee, J. H. Ahn, C. T. A. Brown, W. Sibbett, and A. C. Ferrari, Appl. Phys. Lett. **102**, 013113 (2013).
[32] M. N. Cizmeciyan, J. W. Kim, S. Bae, B. H. Hong, F. Rotermund, and A. Sennaroglu, Opt. Lett. **38**, 341–343 (2013).
[33] I. H. Baek, S. Y. Choi, H. W. Lee, W. B. Cho, V. Petrov, A. Agnesi, V. Pasiskevicius, D.-II. Yeom, K. Kim, and F. Rotermund, Opt. Exp. **19**, 7833–7838 (2011).
[34] W. B. Cho, J. H. Yim, S. Y. Choi, S. Lee, A. Schmidt, G. Steinmeyer, U. Griebner, V. Petrov, D.-I. Yeom, K. Kim, and F. Rotermund, Adv. Funct. Mater. **20**, 1937–1943 (2010).
[35] W. B. Cho, A. Schmidt, S. Y. Choi, V. Petrov, U. Griebner, G. Steinmeyer, S. Lee, D.-II. Yeom, and F. Rotermund, Opt. Lett. **35**, 2669–2671 (2010).
[36] A. Schmidt, P. Koopmann, G. Huber, P. Fuhrberg, S. Y. Choi, D.-I. Yeom, F. Rotermund, V. Petrov, and U. Griebner, Opt. Exp. **20**, 5313–5318 (2012).
[37] H. Yu, X. Chen, X. Hu, S. Zhuang, Z. Wang, X. Xu, J. Wang, H. Zhang, and M. Jiang, Appl. Phys. Exp. **4**, 022704 (2011).
[38] Q. Wang, H. Teng, Y. Zou, Z. Zhang, D. Li, R. Wang, C. Gao, J. Lin, L. Guo, and Z. Wei, Opt. Lett. **37**, 395–397 (2012).